Optical Model-Driven Sharpness Mapping for Autofocus in Small Depth-of-Field and Severe Defocus Scenarios

Supplementary Material

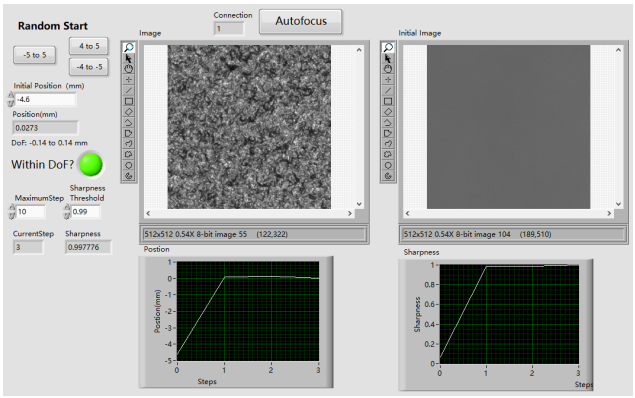

Figure 1. Interface of the autofocus test program. LabVIEW is used for data acquisition, with communication to the Python program via the TCP protocol. The right side shows the image at the initial position.

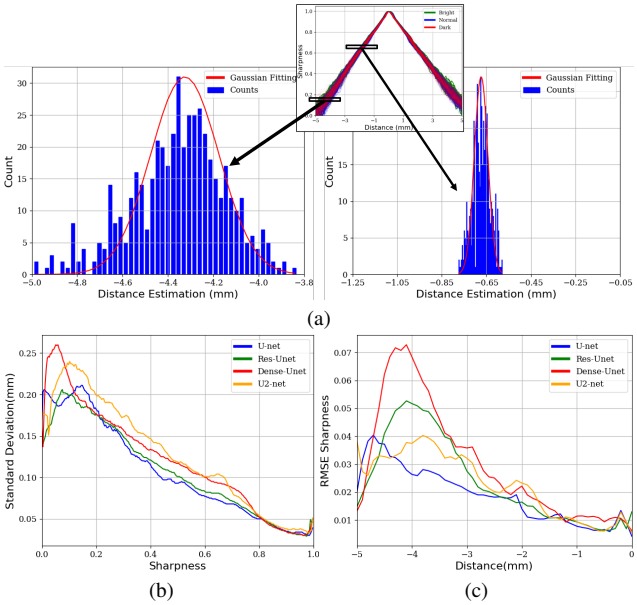

Figure 2. (a) Deviation of distance estimation. The Y-axis means the number of prediction results at a certain range. (b) STD of distance estimation. (c) RMSE of Flat Samples.

1. Deviation of Sharpness Curves

This section presents additional results on distance and sharpness estimation, focusing on the standard deviation (STD) and root-mean-square error (RMSE) of predictions at various positions. Fig. 2a illustrates the deviation observed at both severe and less severe defocus positions. The blue bars represent the distribution of distance predictions for the test samples, while the red line shows the Gaussian fitting curve. As seen, the more severe the defocus, the larger the deviation.

Fig. 2b depicts the relationship between the standard deviation and the focus level. Interestingly, within the in-focus range, where sharpness approaches 1, the distance prediction demonstrates higher uncertainty compared to adjacent positions. This observation highlights that even within the depth-of-field (DoF), the deep learning model struggles to accurately determine the focus level. The drop at the leftmost end of the curve is due to the boundary constraint. Similarly, Fig. 2c reveals a comparable trend. The RMSE of sharpness estimation decreases as the measurements approach the focal plane. The drop at the boundary is again caused by the constraint.

The larger deviation observed in defocused regions necessitates multiple adjustment steps in the proposed autofocus (AF) method. To achieve fewer or one-shot AF system, the deviation of distance estimation must be minimized.

2. Sharpness Consistency

The inconsistency of sharpness values in conventional methods is one of the root causes for the need for peak searching. In comparison, the proposed sharpness method demonstrates outstanding consistency, especially within the in-focus range. Fig. 3c shows the sharpness curve calculated using the conventional squared gradient algorithm [6]. For clarity, we only present results of nine focus stacks under bright, normal, and dark illumination conditions. As illustrated, the sharpness peaks vary significantly across different illumination settings. To measure sharpness consistency, we calculate the ratio of the peak sharpness values, defined as:

$$SR = \frac{S_{peaks}}{min(S_{peaks})} \tag{1}$$

where S_{peaks} represents the peak values of each test focal stack. This metric reflects the relative value of peak sharpness across focus stacks. Fig. 3d shows that, under the conventional method, the in-focus sharpness of bright samples is 3.5 to 4.5 times higher than that of dark samples. Even under the same illumination condition, peak values can vary by more than 20%. This uncertainty creates challenges in identifying the sharpest value in a focus stack.

In contrast, Fig. 3b illustrates the sharpness ratio for the proposed method. It demonstrates that, even under varying illumination conditions, the in-focus sharpness values remain consistent, fluctuating by less than 1%. This feature not only improves AF efficiency but also enables accurate identification of the in-focus region, serving as a reliable stop condition for AF applications.

3. Real Multi-Altitude Samples

This section presents additional features of our method. Using real-world multi-altitude data, which were not part of the training sets. Fig. 4 shows an image alongside its corresponding sharpness map. The anodized samples consist of three distinct flat altitudes. Our proposed method effectively separates these areas and identifies the in-focus region.

This capability has potential applications in auto-labeling for each region of interest (ROI) and enabling AF for each ROI. Each ROI corresponds to a different altitude of the sample, making multi-altitude AF feasible, as Fig. 4a shows.

In addition, the sharpness map demonstrates potential for enhancing focus stacking technology. Focus stacking [1, 4], also known as multi-focus image fusion [2, 3], combines images taken at different focus settings to reconstruct an extended DoF or produce an all-in-focus image. This technique is often used in photography and microscopy applications [4, 5]. Focus stacking typically requires dense sampling to achieve optimal results. By using the sharpness map, the meaningful range for sampling can be located more efficiently, reducing the need for dense sampling. This represents a promising future application of the proposed sharpness estimation method.

4. Sharpness and End-to-End DE

Due to the inherent uncertainty in optical defocus, direct end-to-end distance estimation (DE) models can produce incorrect predictions regarding the direction from the focal plane. In our test sets, approximately 20% of the predictions are observed to be incorrect.

Fig. 5 presents the analysis performed with the scaled optical-based sharpness curve proposed in this study. Correct predictions are marked in blue, while incorrect predictions are highlighted in red. The scaled sharpness curve is represented by the green line. The results show that the end of the incorrect predictions (red points) lies higher than the leftmost end of the correct predictions (blue points). Which is consistent with the optical-based sharpness curve. This trend indicates that the direct end-to-end DE model inherently aligns with the optical-based assumption, further supporting its validity.

These findings demonstrate that our optical model-based approach effectively reduces the uncertainty for deep learning models when learning from defocus images, thereby enhancing autofocus application.

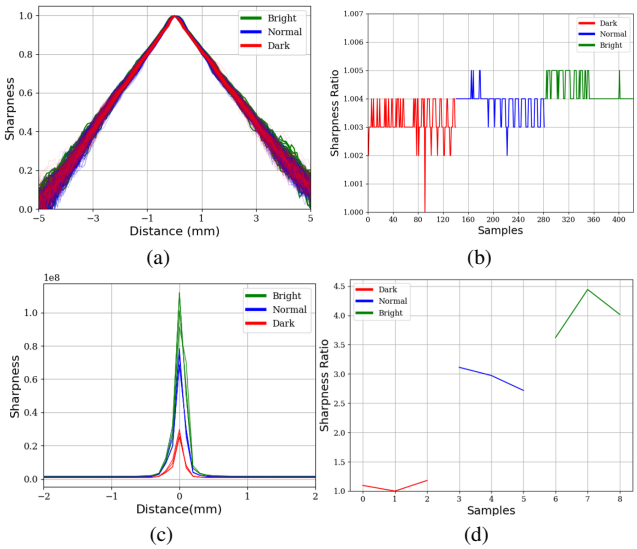

Figure 3. (a) Proposed sharpness curve. (b) Sharpness ratio of the proposed method (c) Conventional sharpness curve by Squared Gradient algorithm (d) Sharpness ratio of conventional method. For visual conciseness we only present 9 samples of conventional.

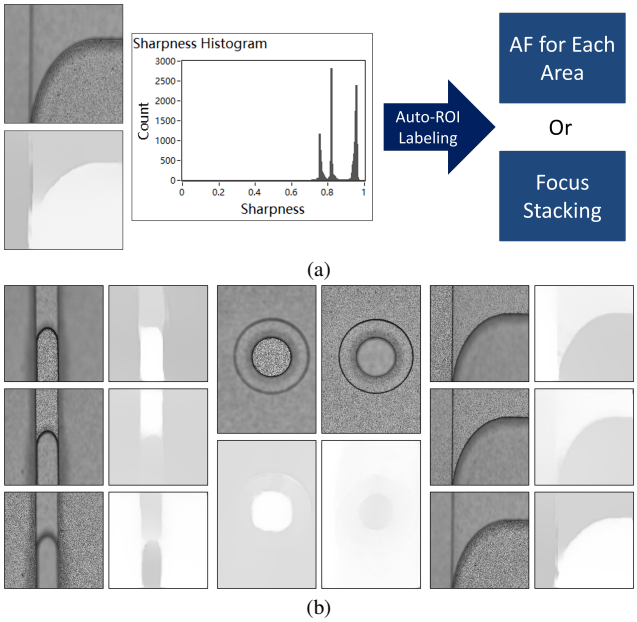

Figure 4. (a)Framework for multi-altitude autofocus(b)Images of real-multi-altitude samples

References

[1] David Choi, Aliya Pazylbekova, Wuhan Zhou, and Peter van Beek. Improved image selection for focus stacking in digital photography. In *2017 IEEE International Conference on*

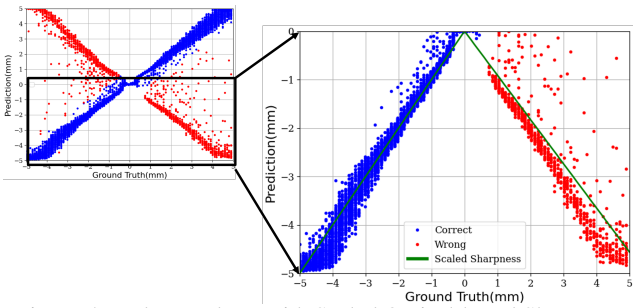

Figure 5. End-to-End DE with Scaled Optical-based Sharpness

Image Processing (ICIP), pages 2761–2765. IEEE, 2017. 2

[2] Paul R Hill, Cedric Nishan Canagarajah, David R Bull, et al. Image fusion using complex wavelets. In *BMVC*, pages 1–10. Citeseer, 2002. 2

[3] Wei Huang and Zhongliang Jing. Evaluation of focus measures in multi-focus image fusion. *Pattern recognition letters*, 28(4):493–500, 2007. 2

[4] Madhu S Sigdel, Madhav Sigdel, Semih Dinç, Imren Dinc, Marc L Pusey, and Ramazan S Aygün. Focusall: Focal stacking of microscopic images using modified harris corner response measure. *IEEE/ACM Transactions on Computational Biology and Bioinformatics*, 13(2):326–340, 2015. 2

[5] Yu Song, Mantian Li, Qingling Li, and Lining Sun. A new wavelet based multi-focus image fusion scheme and its application on optical microscopy. In *2006 IEEE International Conference on Robotics and Biomimetics*, pages 401–405. IEEE, 2006. 2

[6] Yu Sun, Stefan Duthaler, and Bradley J Nelson. Autofocusing in computer microscopy: selecting the optimal focus algorithm. *Microscopy research and technique*, 65(3):139–149, 2004. 1